



**HAL**  
open science

# Experimental Uses of Positronium and Potential for Biological Applications

Adrien Hourlier, F. Boisson, D. Brasse

► **To cite this version:**

Adrien Hourlier, F. Boisson, D. Brasse. Experimental Uses of Positronium and Potential for Biological Applications. *IEEE Transactions on Radiation and Plasma Medical Sciences*, 2024, 8 (6), pp.581-594. 10.1109/TRPMS.2024.3407981 . hal-04751608

**HAL Id: hal-04751608**

**<https://hal.science/hal-04751608v1>**

Submitted on 25 Oct 2024

**HAL** is a multi-disciplinary open access archive for the deposit and dissemination of scientific research documents, whether they are published or not. The documents may come from teaching and research institutions in France or abroad, or from public or private research centers.

L'archive ouverte pluridisciplinaire **HAL**, est destinée au dépôt et à la diffusion de documents scientifiques de niveau recherche, publiés ou non, émanant des établissements d'enseignement et de recherche français ou étrangers, des laboratoires publics ou privés.

# Experimental uses of positronium and potential for biological applications

A. Hourlier<sup>1,2</sup>, F. Boisson<sup>1,2</sup> and D. Brasse<sup>1,2</sup>

<sup>1</sup> Institut Pluridisciplinaire Hubert Curien, Université de Strasbourg, 23 rue du Loess 67037 Strasbourg, France

<sup>2</sup> CNRS, UMR7178, 67037 Strasbourg, France

**Abstract**—Positrons are widely used in molecular imaging through the Positron Emission Tomography (PET) imaging technique. However PET only reconstruct the distribution of the positron emitting radioisotopes, and because the  $\beta^+$  isotopes are linked to a vector molecule, the distribution of  $\beta^+$  isotopes is correlated to the distribution of a given biological function.

Positron-electron annihilation can transit through a meta-stable called positronium, which can exist in two spin states : the single state - parapositronium - and the triplet state - orthopositronium. The orthopositronium lifetime ( $\tau_{oPs}$ ), formation probabilities and decay modes are sensitive to the physical and chemical state of the neighboring medium and could therefore provide information on the tissues themselves during a PET acquisition. However, traditional PET only relies on the detection of the two annihilation photons, therefore the lifetime and annihilation higher multiplicity annihilations are not accessible to such PET paradigm.

This review will present some of the use cases of positronium as a specific signature for event selection in astrophysics and particle physics, and as a probe for the microscopic state of materials and tissues. These usages of positronium highlight the interest for positronium for diagnostic in medical science, the projects for using positronium in upcoming PET tomographs are then presented.

**Index Terms**—Orthopositronium, molecular imaging, positronium

## I. INTRODUCTION

Positrons (anti-matter partners of electrons) are widely used in medical imaging, mainly in Positron Emission Tomography (PET). PET is a powerful imaging technique that is used to map biological functions in the subject's body. It relies on the detection of the annihilation of positron from  $\beta^+$  isotopes such as  $^{18}\text{F}$ , associated to a vector molecule. The positrons travel and thermalize across a short distance before annihilating with electrons, resulting, in the majority of cases, in the production of two 511 keV annihilation photons emitted in opposite directions and detected by an array of scintillating detectors surrounding the subject.

The spatial distribution of the annihilations is used to reconstruct a three-dimensional image of the radioactive tracer distribution in the body, highlighting the desired biological functions. PET is particularly useful in oncology [1], [2], as it is used to detect cancerous lesions and monitor response to therapy. It can also be used in pharmacology to study the distribution of new molecules [3], [4], and a recent increase of interest in botanical sciences is observed.

In general, thanks to the nearly endless radiotracer diversity, allowing to study a large array of biological processes, PET is an important quantitative research tool in the clinical and preclinical fields, and more widely, in all areas of life science [5].

Most recent developments in PET are focused on improving detection efficiency and time resolution, both in an effort to improve the overall final image quality. The imaging principle however remains based on reconstructing the topological density of the radiotracer, and the temporal evolution of that distribution. More information can in principle be extracted from the annihilation process itself, that can inform on the chemical and physical state of the biological tissues, although this is not yet taken advantage of in commercial PET systems.

Positron annihilation can transit through a meta-stable bound state called positronium. The positronium state forms singlet (total spin  $S = 0$ ) and triplet ( $S = 1$ ) spin states respectively called para- and ortho- positronium. The parapositronium ( $p$ -Ps) decays primarily to two back-to-back 511 keV photons with a lifetime of 0.125 ns in vacuum, and the orthopositronium ( $o$ -Ps) decays mainly to three photons adding up to two electron masses ( $m_e$ ), with a lifetime of 142 ns in vacuum [6]. However,  $o$ -Ps formation probability, lifetime and decay modes are highly sensitive to the physical and chemical environment, mostly due to pick-off interactions with nearby electrons [7], and conversion and oxydation with surrounding free radicals [8], [9].

In materials science and engineering, the study of positronium formation and annihilation is used as a probe for nano-scale physical and chemical properties of solids and liquids. It is used in wide ranges of applications such as evaluating the micro-porosity of bulk materials [11], the oxygen partial pressure in porous compounds [12], or even the surface tension of molecular liquids [13].

In biology, positronium has been used on small tissue samples to study hypoxia [14]–[16], and the size of free volumes in tumors [17], [18] and blood clots [19]. While these measurements are ways to quantify the physical and chemical state of the tissues, no correlation is yet established to specific biological processes, nor can it yet be used in predictive diagnostics. The promises of using positronium in biological and medical sciences has been highlighted recently [20] and using positronium as an imaging technique is a relatively novel field, proposed by P. Moskal [21]–[23], and gaining a lot of attention over the last few years.

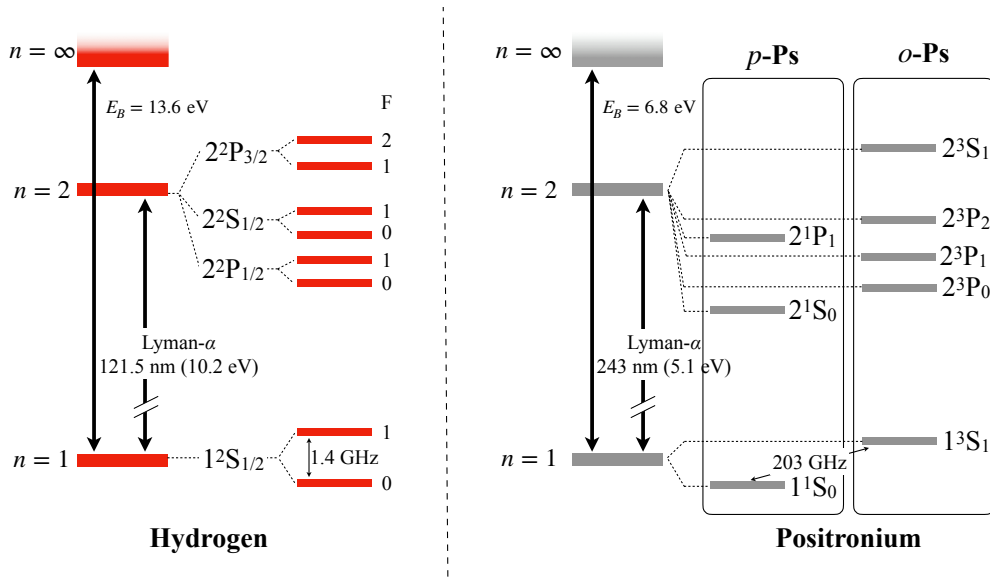


Fig. 1. Hydrogen and positronium energy levels, modified from [10]. The energy levels of positronium are similar to the ones of hydrogen with a factor of two, because of the change in reduced mass of the system, which is  $m_e$  for hydrogen, and  $m_e/2$  for positronium, due to the change of a proton in hydrogen into an positron in positronium.

While positrons used in PET undergo such positronium state, traditional two-photon PET only observes the products of the annihilation of the positron or positronium, and not its formation. It is therefore impossible to evaluate the  $o$ -Ps lifetime ( $\tau_{oPs}$ ). This imaging requires a change in isotope, using  $(\beta^+, \gamma)$  isotopes, including but not limited to  $^{44g}Sc$ ,  $^{72}As$ ,  $^{88g}Rb$ , or  $^{94m}Tc$  [24]–[26], which emit a prompt  $\gamma$  as a marker of the emission of the positron, and therefore would allow to measure  $\tau_{oPs}$ . To this date demonstration of the possibility of performing *in-vivo* imaging with positronium candidate events has been presented by the Jagiellonian PET (J-PET) research group [27], [28], in this case, the average lifetime over the regions of interest delineated by standard PET is used to overcome the low  $(\beta^+, \gamma)$  branching ratio of  $^{68}Ga$  and the large spatial resolution of the J-PET prototype in this acquisition mode.

In the following sections, we will first present the physical properties of positronium in the quantum electrodynamics frameworks and describe the formation and interaction processes. We will then describe the main experimental techniques available to perform positronium studies before focusing on examples of the uses of positronium in various physics fields. Finally, we will present the existing studies of positronium behaviour in biological samples, and the newly proposed field of positronium imaging, introduced in 2018 [21], [23].

## II. FORMATION, INTERACTION AND ANNIHILATION OF POSITRONIUM

The first theoretical discussions of positronium were performed by Pirenne [29], [30] and Wheeler [31]. Positronium was later experimentally evidenced by Deutsch in 1951 by observing the apparition of positronium lifetime in the annihilation time distribution of positrons in gases [32], by observing

a three quanta positron annihilation [33], and by measuring the fine structure resonance between  $p$ -Ps and  $o$ -Ps [34].

### A. Positronium in Quantum Electrodynamics

As the simplest purely leptonic electromagnetically bound state, being composed of two low-mass leptons, positronium is, for all practical purposes, fully described by Quantum Electrodynamics (QED). The absence of hadronic components suggests that positronium energy levels and decay rates can be calculated to very high precision, limited only by the order of the corresponding perturbative expansion, which opens up the possibility to test QED bound-state theory with unprecedented precision.

QED is the most precisely tested theory in physics, and agrees with all observations performed so far, having been tested at the part per trillion level (i.e. parts in  $10^{12}$ ) [10]. Because the theory is so well established it is possible to use precision measurements of Ps to search for effects that may be caused by elements not included in the theory.

Observables of interest for testing QED are energy intervals, measured using laser and microwave spectroscopy, decay rates, measured using positron annihilation lifetime spectroscopy, and decay modes, measured using polarization and momentum measurements to look for forbidden symmetries.

The general selection rule for the annihilation of positronium from a state of orbital angular momentum  $l$  and total spin  $s$  into  $n$  photons is given by  $(-1)^{l+s} = (-1)^n$  [7]. Therefore  $p$ -Ps in a ground state ( $l = 0, s = 0$ ) will decay into an even number of photons while  $o$ -Ps in the ground state ( $l = 0, s = 1$ ) decays in an odd number of photons, greater than one since a single photon decay is forbidden because of momentum conservation.

For positronium formation in an un-polarized medium, the four electron/positron spin states  $|\uparrow\uparrow\rangle$ ,  $|\uparrow\downarrow\rangle$ ,  $|\downarrow\uparrow\rangle$ , and  $|\downarrow\downarrow\rangle$  are

equally probable. Thus the formation of  $o$ -Ps and  $p$ -Ps :

$$o\text{-Ps} = \left\{ |\uparrow\uparrow\rangle; \frac{1}{\sqrt{2}}(|\uparrow\downarrow\rangle + |\downarrow\uparrow\rangle); |\downarrow\downarrow\rangle \right\} \quad (1)$$

$$p\text{-Ps} = \frac{1}{\sqrt{2}}(|\uparrow\downarrow\rangle - |\downarrow\uparrow\rangle) \quad (2)$$

should follow a 3:1 ratio. This ratio has been observed in low density gas, the  $3\gamma:2\gamma$  events ratio (respectively from  $o$ -Ps and  $p$ -Ps annihilation) approaches 3:1 with decreasing gas density, reflecting the statistical ratio of the triplet and singlet states [7].

Positronium energy levels, illustrated in figure 1, are similar to the hydrogen levels scaled by the ratio of reduced masses between hydrogen and positronium. Due to the large difference between the proton and electron masses, the reduced mass of hydrogen is  $\sim m_e$ , where it is  $m_e/2$  for positronium. The energy level of the ground state  $o$ -Ps is higher than that of the ground state  $p$ -Ps due to the spin-spin interaction between the electron and the positron. This difference is called the hyperfine structure of the ground state positronium, which is about 203 GHz [35].

Photons from the annihilation are intricated, with a correlation of their polarization states. This correlation can be found in the angular distribution of their Compton scatters, which can provide an accurate test of Bell's theorem to the possibility of constructing a physical theory that describes the "real factual situation" in the Einstein–Podolsky–Rosen paradox [36]. The polarization of the  $o$ -Ps annihilation photons has been used to perform tests of the P, T and CP invariances in the J-PET tomograph with precision at the order of  $10^{-4}$  [37].

An in depth review of the theoretical fundamental aspects of positronium physics can be found in [38], [39] that covers extensively the QED aspects of the positronium.

The first experimental measurements of  $\tau_{p\text{Ps}}$  found an annihilation rate of  $\Gamma_{2\gamma}(1^1S_0, \text{exp}) = 7.99(11) \times 10^9 \text{s}^{-1}$  (i.e. a lifetime of  $125 \pm 2$  ps) from studying the radio-frequency resonance linewidth as a function of power in a Zeeman experiment and extrapolating to zero power by [40]. First measurements of  $\tau_{o\text{Ps}}$  are performed by measuring  $o$ -Ps annihilation in a moderating gas and extrapolating at zero density, [41] found a rate of  $\Gamma_{3\gamma}(1^1S_1, \text{exp}) = 7.275(15) \times 10^6 \text{s}^{-1}$  (i.e. a lifetime of  $137.4 \pm 0.3$  ns), and [42] found a rate of  $\Gamma_{3\gamma}(1^1S_1, \text{exp}) = 7.262(15) \times 10^6 \text{s}^{-1}$  (i.e.  $137.7 \pm 0.3$  ns). The evolution of  $\tau_{o\text{Ps}}$  measurements is shown in figure 2. It is notable that early measurements of  $o$ -Ps annihilation rates (e.g. from [6] and [42]) deviate from the expected theoretical values, a problem known as the  $o$ -Ps paradox. This was solved in 1995 by using slow positron beams and including higher order corrections to the extrapolations to zero-density media [43]–[45]. The latest measurements for  $p$ -Ps and  $o$ -Ps lifetimes are summarized in table I.

TABLE I  
BEST ANNIHILATION LIFETIME MEASUREMENTS TO DATE FOR PARA- AND ORTHO- POSITRONIUM, COMPARED TO THE THEORETICAL VALUES EXTRACTED FROM [10].

|         | Theoretical value | Measurement       | Rel. precision | Year |
|---------|-------------------|-------------------|----------------|------|
| $p$ -Ps | 125.1624(3) ps    | 125.14(3) ps [46] | 213 ppm        | 1994 |
| $o$ -Ps | 142.0459(4) ns    | 142.04(2) ns [47] | 156 ppm        | 2009 |

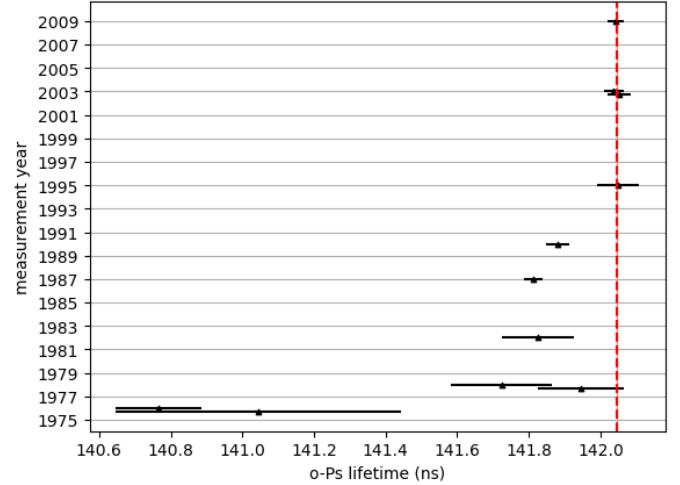


Fig. 2. Evolution of the experimental determination of the vacuum value of  $\tau_{o\text{Ps}}$  compared to the theoretical value. The values are extracted from, in chronological order : [48], [49], [50], [51], [52], [53], [54], [43], [45], [55], [47]

### B. Positronium formation process

In gases, positronium can be formed if the positron kinetic energy  $T$  is in the range  $E_i - E_{ps} \leq T \leq E_i$ , where  $E_i$  is the gas first ionization energy, and  $E_{ps}$  is the positronium binding energy in the ground state (6.8 eV), known as the Ore gap mechanism [7], [56].

In bulk metal, positron annihilate directly with conduction electrons from delocalized Bloch states without forming positronium. Positronium formation is only possible in pores or atomic vacancies [7].

In insulators, when the energy requirements for the Ore gap mechanism are not met, the 'Spur process' can happen, mostly in insulating solids and liquids, positronium can be formed by the capture of an electron in the ionization trail of the positron [57].

Experiments in solids indicate that the positronium work function is negative in most materials, i.e. a strong positronium affinity to low density regions of the materials : free volumes in organic materials, color centers in ionic crystals, and atomic vacancies in metals. In solids, Ps can be found in delocalized quantum states that are repelled by the atomic cores of the host material, which are also the locus of higher electron density, thus where collision probability would be higher. Because they propagate in lower density regions of the material, the thermalization process of positrons is slower than that of the electrons [58], [59].

### C. Positronium interaction with its surrounding

While *o*-Ps has a long lifetime (compared to *p*-Ps) in vacuum of  $\sim 142$  ns, in practice in materials that lifetime is drastically reduced. This is due to the interactions of *o*-Ps with its surrounding medium. The main process of interaction is the “pick-off process” a process in which a positron in *o*-Ps state annihilates during a collision with an atomic electron of the right spin resulting in the vast majority of cases in a  $2\gamma$  decay [7], effectively undergoing direct annihilation with that new electron. The pick-off process may also lead to a  $3\gamma$  decay, but with a much lower probability [20] The probability of undergoing pick-off process in liquids is described by the Ferrell bubble model, depending on the surface tension and the presence of dissolved gas [60]. Other interaction processes include conversion and oxydation, i.e. the interaction with radiolytic products created by the positron during thermalization ( $e^-$ ,  $H_3O^+$ ,  $HO^-$  radicals, free radicals) [8], and oxydation  $O_2$  can oxydize positronium through the process :  $Ps + O_2 \rightarrow e^+ + O_2^-$  Spin exchange by interaction with  $O_2$  (and other paramagnetic molecules) magnetic moment causes an exchange from the *o*-Ps to the *p*-Ps states [9].

Because these interactions involve either direct annihilation of the positron partner in the *o*-Ps or conversion of the *o*-Ps to the *p*-Ps states, which have a virtually null lifetime compared to the orthopositronium lifetime, the overall *o*-Ps lifetime is therefore drastically reduced by the presence of surrounding electrons or radiolytic products. Moreover, since the final annihilation process involves a state that is no longer *o*-Ps, the annihilation to three photons is drastically suppressed in favor to a two-photon annihilation.

In solids, Ps can be found in delocalized quantum states that are repelled by the atomic cores of the host material. In metals, positronium are mostly found in atomic vacancies, and in crystals, they are mostly found in color centers, with lower atomic density. In organic materials, positronium are found in the free volumes, the empty space created by the steric hindrance of large molecules. In each of these cases, the measurement of  $\tau_{oPs}$  and the formation fraction of *o*-Ps can inform on the size of these lower electronic density sites, and their proportion in the bulk of the material. In liquids, the deposited energy during positron thermalization creates nanoscopic cavitation bubbles in which *o*-Ps can be formed, the size of these bubbles depends directly on the surface tension of the liquid and impacts  $\tau_{oPs}$ . As such, *o*-Ps formation and annihilation can be considered a probe of the free volumes and vacancies in a material at the nanometer level. The relationship between the average size of the vacancy and the *o*-Ps lifetime is modeled by the Tao Eldrup model [61], [62] :

$$\tau_{oPs}^{-1} = 2 \left[ 1 - \frac{R}{R + \Delta R} + \frac{1}{2\pi} \sin \left( \frac{2\pi R}{R + \Delta R} \right) \right] (\text{ns}^{-1}) \quad (3)$$

where  $R$  is the characteristic radius of the inter-molecular voids in a material, assuming a spherical void shape, and  $\Delta R = 1.66 \text{ \AA}$  is obtained by fitting the observed lifetimes for molecular liquids of various surface tensions [63].

## III. EXPERIMENTAL TECHNIQUES FOR STUDYING POSITRONIUM ANNIHILATION

### A. Positron annihilation lifetime spectroscopy (PALS)

The lifetime of the positron in a medium can be accessed by the time delay between the emission of the positron and the detection of the annihilation photons. The positron emission can be detected by several means, either by the detection of a prompt gamma from the nuclear relaxation of the daughter nucleus in the  $\beta^+$  decay, or by the detection of the scintillation signal of the positron in a scintillating medium, or by the detection of the Cherenkov light for medium with high enough optical index that the positron is emitted above the Cherenkov threshold. The number of annihilation photons can vary depending on the annihilation process and the formation of *o*-Ps or *p*-Ps. The total energy sum of the photons in coincidence should be  $2 \times m_e c^2$ , however some experimental setup rely only on the detection of 511 keV photons, in which case the collection of only one of the photons with the correct energy is enough to detect the positron annihilation.

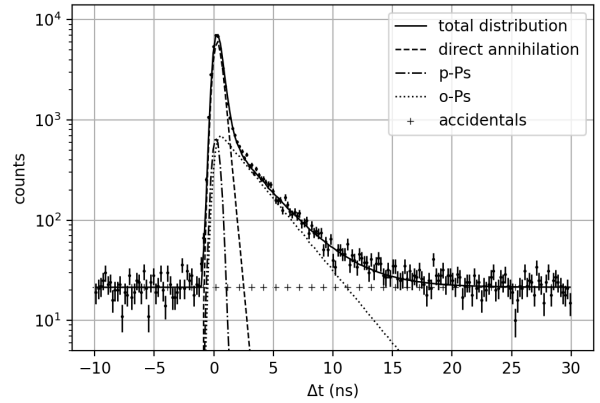


Fig. 3. Example of simulated time distribution of the delay between prompt gammas and annihilation photons ( $\Delta t$ ) used to study positronium formation and lifetime. If positronium is formed, at least three exponential contributions are found : direct annihilation (dashed line), *p*-Ps (dash-dotted line) and *o*-Ps (dotted line). Since  $\tau_{oPs}$  is sensitive to the surrounding medium, multiple  $\tau_{oPs}$  can in principle be measured if enough material variabilities are present. The full distribution (solid line) is also composed of a constant background from random coincidences (cross-signed line), and is convoluted with the time resolution function of the experimental apparatus used to perform the measurement, here modelled by a 500 ps full width half maximum Gaussian.

Figure 3 shows the distribution of time delays between the prompt gamma from  $^{22}\text{Na}$  decays and the detection of positron annihilation photons. The distribution can be described by the sum of three or more exponential contributions, corresponding to the direct positron annihilation, and the formation of *p*-Ps and *o*-Ps :

$$f(t) = \begin{cases} \tau_{\text{Acc}} + \sum_i I_i \frac{1}{\tau_i} e^{-t/\tau_i}, & \text{if } t > 0 \\ \tau_{\text{Acc}}, & \text{otherwise} \end{cases} \quad (4)$$

where  $\tau_{\text{Acc}}$  is the accidental coincidence rate,  $I_i$  and  $\tau_i$  are the relative intensities and lifetimes of the various annihilation processes. Because of the time resolution of the experimental apparatus this distribution is convoluted to the resolution

function  $P(t)$  of the system. The count rate can therefore be expressed as :

$$N(t) = \int_0^{\text{inf}} P(t-x)f(x)dx \quad (5)$$

Typical values to report during a PALS study are the lifetimes and intensities for each annihilation process. The lifetimes can be linked to the size of free volumes through the Tao-Eldrup model from Eq. 3.

### B. Coincidence Doppler Broadening Spectroscopy (CDBS)

CDBS is the measurement of a broadening of the energy spectrum of the true coincidence of two 511 keV annihilation photons beyond the energy resolution of the spectrometer, which provides information on the positron or positronium momentum at the moment of annihilation, as well as information on the momentum of the electron it annihilated with [12], [64]. Since the momentum distribution depends on the site of annihilation, the chemical environment of positron annihilation sites can be appropriately identified by CDBS technique. Two momentum regions are identified in a  $(E_1 - E_2)$  plot, where  $E_1$  and  $E_2$  are the energies of each annihilation photons in the coincidence, as illustrated in figure 4 :

- S region : a region at low momentum around the annihilation peak, which reflects the contribution of positron annihilation by free and valence electrons. This parameter depends on factors such as direct (free positrons) or indirect (Ps formation) annihilation, probability of positron trapping, and density of the sample and its morphology.
- W region : a higher momentum region, on each side of the annihilation peak, typically, which relates to the positron annihilation by core electrons.

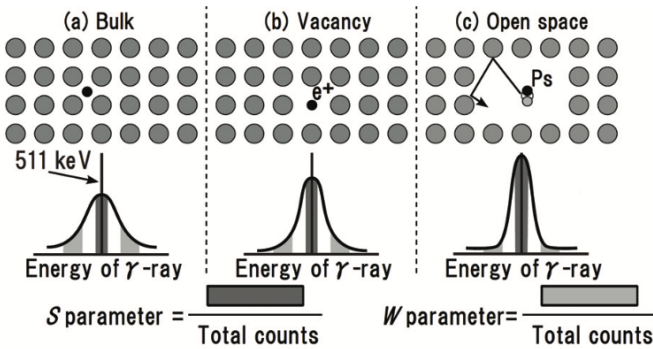


Fig. 4. Schematic summarizing the impact on medium vacancies on the energy difference spectrum between the two annihilation photons, and materializing the regions that enter in the computation of the  $S$  and  $W$  parameters. figure extracted from [64] with the agreement of the publisher.

For example, in [65] sets requirements for the  $S$  parameter of a difference of less than  $3 \times 10^{-3} m_e c^2$  between the two photon energies and for the  $W$  parameter, the energy difference between the two photons needs to lie in the two bands within a  $10$  to  $25 \times 10^{-3} m_e c^2$  on each side of the central energy peak at  $E_1 - E_2 = 0$ . It is to be noted that these numerical values are examples and depend on the studied materials and detector resolution, they are not fixed a priori by physics. While PALS

is most sensitive to the size of elementary free volume, CDBS allows to evaluate the positronium chemical interaction with its environment, by providing a ratio of annihilations with valence or core electrons.

### C. Angular correlation of annihilation radiation (ACAR)

ACAR investigates the electronic band structure of materials such as metals, alloys and semiconductors [66], [67]. In two quanta annihilations, the two annihilation photons are emitted in exactly opposite directions in the frame of the positron-electron pair. In the laboratory frame, a small angular deviation from  $\pi$  of  $\theta = p_t/m_e c$  is observed, originating from residual transverse momentum  $p_t$  of the electron-positron pair or of the positronium at the moment of annihilation, where the momentum  $\vec{p}$  can be written as the sum of longitudinal momentum  $\vec{p}_l$ , along the emission direction of the photons, and  $\vec{p}_t$  the transverse momentum. The width of the peak around  $\theta = \pi$  provides information on the typical energy of electrons and positrons, and additional peaks at higher values of  $\theta$  provide information on the lattice reciprocal vector, in the case of well-defined crystalline structures.

Because ACAR relies on the assumption that two photons are emitted, only direct annihilation and  $p$ -Ps annihilation are detectable, the three quanta annihilation from  $o$ -Ps is not usable, however the two-photon annihilation resulting from  $o$ -Ps interactions with its surrounding is. The momentum distribution of the center of mass in direct annihilation is shifted towards higher values than that of the  $p$ -Ps, leading to a broader ACAR distribution for direct annihilation than for  $p$ -Ps formation.

When PALS provides a measurement of the size of free volumes, and CDBS provides information on the energy of the interacting electrons, the ACAR technique provides complementary information about the shape and periodicity the free volumes in materials [68]. This provides valuable information on crystals, but also on metals or materials with periodic electronic band structures.

## IV. POSITRONIUM IN MATERIALS SCIENCE

One of the major use of positronium is the study of material structure through PALS. The orthopositronium lifetime and production probability is used to probe the size of free volumes at the molecular level on the surface layer of materials. Then the size of free volumes is linked to various material properties (porosity, structural defects, ...), or environmental variables such as humidity or temperature. While listing all studies using this measurement is beyond the scope of this review, we present below a few examples of its use cases.

Studies have shown a reduction of  $\tau_{oPs}$  in solids and liquids with temperature and pressure as the free volume size is reduced [69]. Positronium formation in metals and crystals from slow positron beams has been used to study defects in the structure [11], [70], [71], although [71] pointed out the limitation of this technique for metals since positrons do not propagate in metals, due to the high probability of undergoing direct annihilation with one of the free conduction electrons, only the few tens of nanometers of the surface can be probed.

The porosity of materials can be evaluated by PALS through the correlation of  $\tau_{oPs}$  with pore size: although pores are not empty volumes, they are filled with gas, much less dense than the surrounding material, i.e. with a lower electronic density for positronium to interact with. This is used to study the density of aerogels [12], [72], [73], the pore sizes in silica film [74] and the free volume changes of nanopores in nanostructured  $MgAl_2O_4$  ceramic materials [75].

A study over various organic liquids (benzene, n-hexane, TMS, methanol, ethanol, n-butanol, n-hexanol, n-octanol, and water as a reference) found a correlation between the electronic polarizability of the molecules and the lifetime of free positrons (from direct annihilation), and a correlation between the square root of the surface tension and the lifetime  $\tau_{oPs}$  of orthopositronium from pick-off process [76]. Organic solids, such as polystyrenes, offer a few well defined free volumes repeated throughout the material, it is therefore possible to fit multiple values of  $\tau_{oPs}$  from a given volume [77] corresponding to these well defined sizes.

For studies in material sciences, where no biological information is sought, positrons are usually emitted from a  $^{22}Na$  source directly adjacent to the material sample to be studied, or a beam of cold positrons is employed, to better constrain the depth of penetration of the positrons in the materials and study the structure of samples at given depths. In that latter case, positrons emitted from a source are reflected by a metallic surface at thermal temperatures, and accelerated by a electrostatic accelerator to desired energies [7]. Conversely to PET imaging where a vector molecule is required to bring the radioisotope to a given part of the body expressing a desired biological function, in the case of materials science no topological information is required, therefore no vector is needed.

Finally, in more complex bio-mimetic materials such as phospholipids, the increased packing achieved through self assembly modifies the amount of free volumes and PALS can be used to measure phase transitions in the molecular chain assembly [78].

## V. POSITRONIUM IN EXPERIMENTAL ASTRO- AND PARTICLE-PHYSICS

In astrophysics, positronium formation in galactic gases is studied by comparing the red-shifted 511 keV  $\gamma$  line, evidence of direct positron annihilation and  $p$ -Ps formation, to the lower energy  $\gamma$  continuum, indicating of  $o$ -Ps  $3\gamma$  decay [79].

A more confidential use of orthopositronium is its use in neutrino physics. Detection of electron anti-neutrinos from nuclear reactors and  $\beta$  decays in geologic layers (geo-neutrinos) is achieved through the inverse beta decay reaction  $\bar{\nu}_e + p \rightarrow n + e^+$ . Events are selected based on the double coincidence of a prompt signal (positron scintillation and annihilation) and the delayed neutron capture. Separation between neutrino events and  $(\beta, n)$  decays from cosmogenic-generated radio-nuclides such as  $^9Li$  or  $^8He$  in organic liquid scintillator-based detectors is not possible in an event by event basis unless a distinction between electrons and positrons can be achieved. While the positronium lifetime is typically too

short for neutrino detectors to separate the photons from the positron scintillation from those from the 511 keV annihilation photons, a modification of the scintillation pulse shape can be observed when  $o$ -Ps is formed compared to the scintillation of an electron, or when  $p$ -Ps is formed [80], [81].

The event-by-event  $o$ -Ps selection have been used in the Double Chooz reactor neutrino experiment [82] and is proposed for the upcoming JUNO [83] experiment, to obtain a lower-statistic but cleaner sample of neutrinos, in order to better evaluate backgrounds in their full statistic neutrino selection. The Borexino experiment also used  $o$ -Ps to statistically evaluate their backgrounds [84].

Solar neutrino experiments rely on the measurement of electron recoil during neutrino elastic scattering on an electron. An important background in these neutrino search comes from  $\beta^+$  decays in the detector, mostly from  $^{11}C$ . In these cases orthopositronium tagging can be used to reduce the background [84].

## VI. STUDIES OF POSITRONIUM IN BIOLOGICAL SAMPLES

Positrons used in biology and medicine are confined to their use in PET as far as imaging techniques go, but PALS has been applied to a few biological samples, highlighting correlations between lifetime modifications and various characteristics of the studied sample.

Free volume voids play a key role in dynamic processes in biological systems, including permeability of small molecules, and diffusion of drugs through cell membranes [85]. The PALS technique, by allowing a direct estimation of free void sizes, is critical to understand physical and mechanical properties of complex systems such as collagen [86], porcine eye lens [87], rat brain sections [88], and human skin [89]–[92]

Tracking the changes of the relative weights of  $o$ -Ps interactions with its surrounding, through modification of  $\tau_{oPs}$  or through the  $3\gamma/2\gamma$  ratio, has been used to evaluate the change in void size in treated and un-treated tumors such as in colonic adenocarcinoma [17] and as a marker for cellular hypoxia [14], [16]. However, inside biological materials, the picture is more complicated than in materials science. Defects and free volumes are not homogeneously spread throughout the material. Moreover, the coupling of positronium states to the surrounding material can occur with a wide variety of molecules, and the local chemistry also plays a role, along with the size of free volumes. In that setting, positronium lifetime and formation probability depend on the healthiness of the material, its nanostructure and concentration of bio-active molecules. These factors are indicative of the stage of development of metabolic disorders of tissues. It is therefore believed that positronium decay can provide new input in medical diagnosis.

$o$ -Ps have been used on vegetal tissues, for example to study the microstructure in seeds [93], [94] or the decomposition of starch [95]. Correlations between free volume size and lead concentration in the tissues have been studied by [96].

Positronium has also been used to investigate animal tissue. Slow positron beams have been used to study in-situ the impact

of humidity of mouse skin [92]. A decrease of positronium lifetime and an increase of production intensity is observed with the incident positronium energy of slow positron beams. This effects reaches asymptotic behaviour at positron energies above 5 keV [97]. This dependency has a negligible impact for studies using radioactive positron sources such as  $^{22}\text{Na}$  or  $^{44}\text{Sc}$ , which produce positrons up to  $\sim 1.2$  MeV.

Studies on rat brain sections with and without tumor [88] pointed out the problem of subject-to-subject and organ-to-organ variability preventing from establishing a clear universal  $\tau_{o\text{-Ps}}$  measurement. For a given subject however, a systematic decrease of  $\tau_{o\text{-Ps}}$  between healthy and pathologic tissues is found, indicating that a relative  $o\text{-Ps}$  measurement could be used in future diagnostics.

Positronium lifetime in porcine eye lens [87], [98] shows a correlation with temperature of the tissue sample. Pathologies often imply an elevation of temperatures that can modify the physical structure of the tissues.

PALS was used on human muscles to demonstrate that water in the cells is in liquid form rather than in micro-crystals [99]. The first PALS study on live human cancer cells was performed on 3D carcinoma cell cultures, showing the difference of free voids in the cultures treated or not with a transforming growth factor  $\beta$  (TGF- $\beta$ ), showing the impact on cellular growth medium on the development of the culture and demonstrating the ability of PALS to detect such changes [17]. Cellular culture models such as 3D spheroids are a useful tool to study  $o\text{-Ps}$  [100], and to better understand the information that a PALS study can yield and its importance in medical diagnostics. Cancer cells are known to over-express cellular markers such as HER2 [101], [102] on their membrane, which creates free volumes near the cell through steric hindrance. A measure of  $\tau_{o\text{-Ps}}$  modification could allow to measure this excess and help in the diagnostic. A  $^{44}\text{Sc}$ -labelled tracer for studying HER2 expression of cancer cells has already been studied [103], making this a realistic use of PALS for cancer diagnostic [20]. Similarly, the decrease of free volume size for the TNF- $\beta$  cellular receptor compared to the TNF- $\alpha$  has been linked to its increased cytotoxicity for forming necrosis in tumors [104]. PALS can also be used to distinguish between different types of soft tissues, such as leiomyomas and normal myometrium tissues on *ex-vivo* samples [105], or cardiac myxoma and adipose tissues [18], [106].

PALS studies on human skin cancerous samples with squamous cell carcinoma and basal cell carcinoma show a decrease of  $\tau_{o\text{-Ps}}$  of similar magnitude, but the most significant difference with healthy skin sample is the decrease of  $o\text{-Ps}$  formation probability, which allows to distinguish between samples of healthy skin, squamous and basal cell carcinomas [91]. However, melanoma samples present no significant differences with healthy samples for positron beam energies above 2 keV [90], which could be attributed to the lower concentration of melanoma cells in the sample than in the case of squamous and basal cell carcinoma samples, or to the

fact that melanoma cells do not present a significant physical or chemical change compared to healthy skin cells.

PALS measurement on human hair have demonstrated the ability of PALS to provide information on UV-induced hair damage at molecular level for virgin and bleached [107], an important input for cosmetic industry. The bleached hair undergoes photodamage faster in comparison with the virgin hair. PALS can also be used to study the diffusion time of commercial dyes in the porous network of free volumes in the hair [108]. The lifetime decreases up until complete absorption of dye in the hair, then reaches a plateau as all available free volume is occupied.

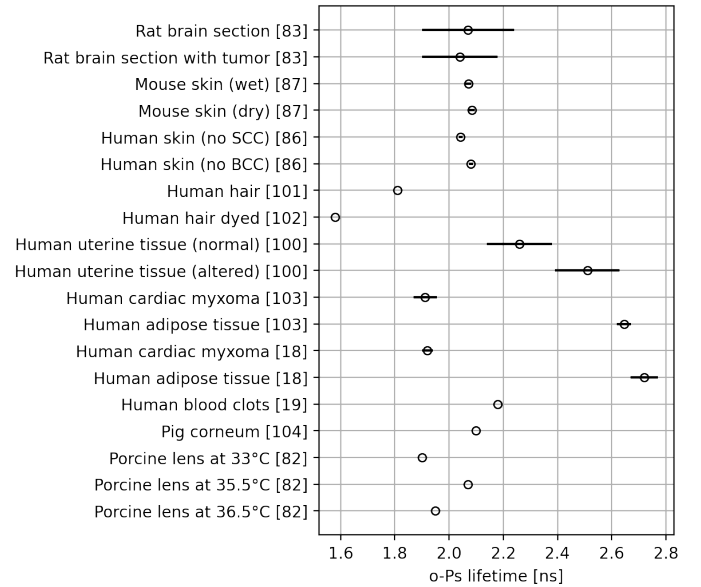


Fig. 5.  $o\text{-Ps}$  lifetime in various biological tissues, ranging from  $\sim 1.6$  to  $\sim 2.8$  ns, values compiled from [18], [19], [87], [88], [91], [92], [105]–[109]

## VII. POTENTIAL APPLICATIONS OF ORTHOPOSITRONIUM IN MEDICAL IMAGING

Positronium formation can be used in PET as a way to select a lower-statistic but purer sample of events, with spatial information from the three-quanta decay of  $o\text{-Ps}$ , allowing to perform PET imaging with enhanced spatial information, or as a way to probe the physical and chemical properties of the tissues in which the annihilation occurs from positronium lifetime imaging.

### A. $o\text{-Ps}$ decay : $3\gamma$ annihilation

The three annihilation photons from  $o\text{-Ps}$  annihilation originate from the same point in space and time. It is therefore possible to extract the position of the emission on an event-by-event basis where traditional  $2\gamma$  PET can only procure a line

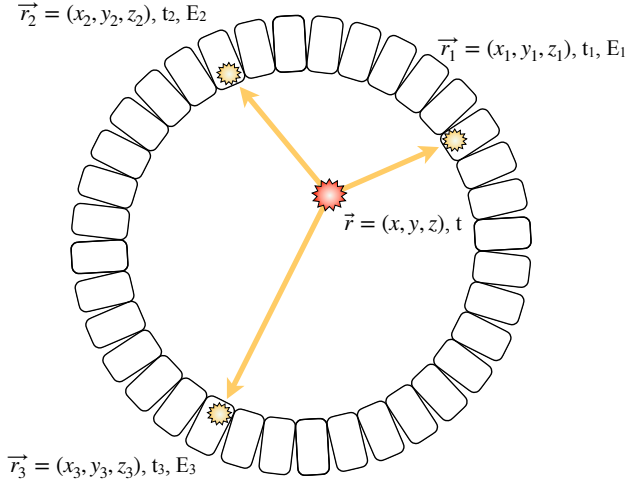


Fig. 6. Schematic representation of the annihilation localization in  $3\gamma o\text{-Ps}$  annihilation imaging, defining the variables necessary for event reconstruction.

of response. In order to satisfy the momentum conservation, the photons must satisfy the following conditions [110], [111]:

$$\begin{aligned}
 p_x &= \sum_{i=1}^3 \frac{E_i}{c} \frac{x - x_i}{|\vec{r} - \vec{r}_i|} = 0, \\
 p_y &= \sum_{i=1}^3 \frac{E_i}{c} \frac{y - y_i}{|\vec{r} - \vec{r}_i|} = 0, \\
 p_z &= \sum_{i=1}^3 \frac{E_i}{c} \frac{z - z_i}{|\vec{r} - \vec{r}_i|} = 0, \\
 E_1 + E_2 + E_3 &= 2 \times m_e c^2 \simeq 1022 \text{keV} \quad (6)
 \end{aligned}$$

where  $\vec{r}$  represents the annihilation location,  $\vec{r}_{i=1,2,3}$  the position at which each of the three photons is detected with an energy  $E_i$ . Here we assume that the positronium annihilation occurs at rest, or with a negligible residual momentum. A residual momentum would yield a non-planarity of the three emitted photon directions. Solving this set of equations with the  $\vec{r}_i$  known to the intrinsic resolution of the detectors allows to reconstruct the  $\vec{r} = (x, y, z)$  position of the annihilation. Here the limiting factor on the spatial resolution of the reconstructed point is the finite energy resolution of the detectors. An energy resolution of a few percents is required to produce usable images, which is rarely the case of scintillator based tomographs. This approach, however, can be envisioned with semi-conductor based PETs such as cadmium zinc telluride (CZT) detectors which can reach 1 – 7% energy resolution at 511 keV [112]–[114], but with worse time resolution than scintillator-based detectors.

Another approach, for worse energy resolution, but better time resolution, detectors, is to perform tri-lateration [115] :

the three photons are emitted at the same time  $t$ . A time of flight analysis allows to locate decays on an event-by-event basis.

The positions and time of detection of each photons need to satisfy :

$$(x - x_i)^2 + (y - y_i)^2 + (z - z_i)^2 = c^2(t - t_i)^2 \quad (7)$$

Moreover, the three annihilation photons are emitted in a plane, which allows to constrain the position of the searched annihilation to the plane containing the three photodetections, reducing the problem to an effectively 2D reconstruction. This is one of the proposed approaches for positronium-based reconstruction in the J-PET tomograph.

While this technique has the advantage of event-by-event annihilation localization, and the use of triple coincidence reduces greatly the noise linked to random coincidences, the  $3\gamma$  annihilation mode is a rare occurrence, since it only occurs in  $o\text{-Ps}$  decay, if no pick-off, nor oxydation, nor conversion happened, and to some fraction of direct annihilation. Even in the case where  $o\text{-Ps}$  is formed, any interaction of  $o\text{-Ps}$  with the surrounding material will result in a  $2\gamma$  annihilation. The count rate for such an imaging mode is expected to be low and require either a very high activity injected to the patient, or a very long acquisition time. Simulations performed assuming the final configuration and performance of the J-PET prototype yield a resolution (RMS) of 2.1 cm for the X and Y coordinates (transaxially with respect to the tomograph) and 2.3 cm for the Z coordinate (axially), with the main limiting factor for the resolutions being the time resolution of the system [115]. Using this method, J-PET has performed the first experimental  $3\gamma$  images of the walls of a cylindrical vacuum chamber at the center of which a point-like  $^{22}\text{Na}$  source is placed [116]. The spatial resolution in that case depends on the temporal resolution of the PET, typically of the order of 250 ps at the time this review is written, but in constant improvement, partly driven by the 10 ps challenge [117].

Another advantage of being able to exploit the  $3\gamma$  decays to perform an image is to then perform the same image with the standard  $2\gamma$  PET, then the voxel-to-voxel ratio of  $3\gamma/2\gamma$  annihilations informs on the annihilation medium.

### B. 3D in-vivo PALS imaging with $(\beta^+, \gamma)$ isotopes

Positron emission tomographs rely on the detection of annihilation photons in order to reconstruct the biodistribution of the radiotracer in a subject. Because no information is provided on the decay time, PETs are unable to perform PALS-like studies under the current paradigm. A considerable amount of information, encoded in the annihilation process, is therefore lost, such as free volume size or chemical composition of the tissues. In order to perform PALS-like studies, a prompt  $\gamma$ , correlated to the positron emission is required. Changing the isotope from  $\beta^+$  to  $(\beta^+, \gamma)$  where the relaxation of the daughter nucleus produces a prompt  $\gamma$  within a few picoseconds of positron emission from the  $\beta^+$  decay, allows to solve this issue.

There are several potential  $(\beta^+, \gamma)$  isotopes that would be suited for positronium imaging [24]–[26], however the best

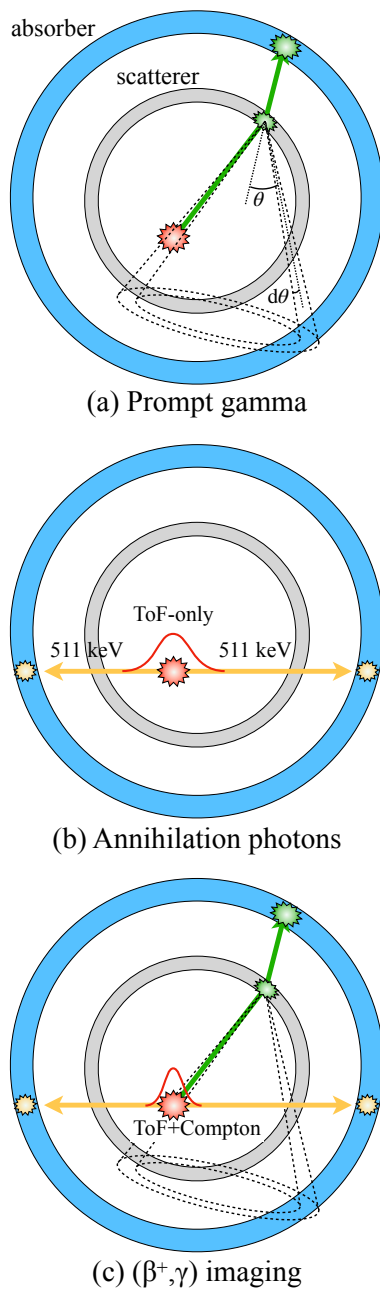


Fig. 7. Annihilation localization in  $(\beta^+, \gamma)$  imaging. (a) The incident direction of the prompt  $\gamma$  can be estimated thanks to the Compton scatter information between the scattering and the absorber layers to a probability Compton cone. (b) The detection of the two annihilation photons define a line of response as is usual in  $2\gamma$  PET. The localization of the annihilation can be improved from being completely delocalized on the line from using time of flight (ToF) information. (c) The intersection of the line of response and the Compton cone enhances the resolution on the annihilation localization that would be provided with only ToF on the line of response.

candidate seems to be  $^{44g}\text{Sc}$  which has a lifetime realistically suited to perform molecular imaging [24], [118]. Furthermore,  $^{44g}\text{Sc}$ -radiolabelled tracers are already developed [119] and many biodistribution studies with  $^{44g}\text{Sc}$  labelled DOTA-peptides have been performed [120]–[128]. Other isotopes are considered, such as  $^{124}\text{I}$  and  $^{66}\text{Ga}$  which have vector

molecules allowing to study genome instability, the expression of specific surface agents or to induce angiogenesis and could be of interest for positronium lifetime imaging of the tissues surrounding the regions expressing these biological functions [129].

A particular issue with relying on triple coincidence events from  $(\beta^+, \gamma)$  isotopes is that while the two annihilation photons are collinear, the prompt  $\gamma$  is emitted in a completely un-correlated direction. So while detecting the second annihilation photon provided that one is detected is only a matter of cross section, not solid angle, the detection of the prompt  $\gamma$  add the inefficiency linked to the solid angle a second time. The coincidence count rate for a  $2\gamma$  detection is proportional to  $\epsilon_{\Omega}\epsilon_{\sigma_1}\epsilon_{\sigma_2}$ , where  $\epsilon_{\Omega}$  is the detection solid angle, and  $\epsilon_{\sigma_1}$  and  $\epsilon_{\sigma_2}$  are the probabilities that the photons 1 and 2 will interact in the crystals they cross, and the count rate for a prompt  $\gamma$  and 2 annihilation photons is proportional to  $\epsilon_{\Omega}^2\epsilon_{\sigma_1}\epsilon_{\sigma_2}\epsilon_{\sigma_p}$ , where the new term  $\epsilon_{\sigma_p}$  corresponds to the interaction probability of the prompt  $\gamma$ . An increase of detection solid angle of the tomograph is crucial to keep an event rate high enough to reconstruct an image. While the overall efficiency to detect  $3\gamma$  events is approximately 10 times lower than that of  $2\gamma$  events, a the gain in solid angle from a full body scanner can overcome that effect and actually provide a better efficiency than a standard  $2\gamma$  acquisition on a 20 cm axial field of view PET scanner [129]. This issue is addressed by the development of total-body PET [130] such as the uExplorer [131], the PennPET explorer [132], Siemen's Biograph Vision Quadra [133], and the J-PET [134], [135] tomographs.

Even with the advent of full body scanners, the  $(\beta^+, \gamma)$  imaging technique is orders of magnitude more efficient than the detection of  $3\gamma$  annihilation for several reasons [20]: first, in the tissues, due to interactions with the surrounding medium,  $o\text{-Ps} \rightarrow 2\gamma$  is about 70 times more probable than  $o\text{-Ps} \rightarrow 3\gamma$ , second, the attenuation, or partial attenuation of  $3\gamma$  events in the body is much larger than the  $2\gamma$  annihilation, because of the higher number of photons and because of their lower energies increasing the interaction probabilities. Finally, the detection efficiency of  $3\gamma$  is lower than the for  $2\gamma$ . This efficiency gap between the two imaging techniques is a major criterion to explain the preference of the  $(\beta^+, \gamma)$  PALS technique for positronium imaging in [106].

The full body coverage of the uExplorer PET/CT is achieved by assembling eight conventional PET rings composed of modules of LYSO (Lutetium Yttrium Orthosilicate) crystal matrices. This provides all the advantages of LYSO:Ce crystals for the detection of 511 keV annihilation photons, especially a high detection efficiency, while offering the many advantages of full body coverage in terms of possible clinical studies [136], [137].

The J-PET tomograph [134], [138], [139] on the other hand is designed as a succession of plastic scintillator strips axially distributed around the patient and read out at both

ends by PMTs. The advantage is that an increase of coverage to a full body PET does not imply an increase of the number of read out channels which only depends on the section of the tomograph, while in the case of the uExplorer, the number of read out channels grows as the surface of the tomograph. However, the low interaction cross section of plastic scintillator imposes the need for a thick detection material, which means many strips on the radial direction. It is also to be noted that in organic scintillators, the primary mode of interaction for photons in the 100 keV to MeV energy range is Compton interaction, which not only allows for detection of the 511 keV photons, but in principle brings new information on the incident direction of the photons, useful to reduce noise when pairing two detections in a coincident event.

The XEMIS and XEMIS2 prototypes [140]–[142] are liquid xenon time projection chambers, they rely on the detection of the triple coincidence of the prompt  $\gamma$  and the reconstruction of the two annihilation photons. The ability to reconstruct the succession of Compton and photoelectric interactions allows these detectors to predict a cone of incident direction for the prompt  $\gamma$ . This detection mode relies on the use of  $^{44g}\text{Sc}$ , but no imaging was performed with the reconstruction of positronium lifetime. As illustrated in figure 7, the directionality of the prompt  $\gamma$  reconstruction allows to improve the localization of the decay along the line of response by the intersection of the line of response with the Compton incident direction cone [143], [144].

Other prototypes plan on using the prompt gamma from the  $(\beta^+, \gamma)$  annihilation to improve on the decay localization [145], which could in time have the capabilities to study  $\tau_{o\text{Ps}}$  in vivo. This prototype uses a first pixellated scattering inner layer surrounded by a pixellated absorber layer. A coincident hit in the scattering layer and in the absorber layer with time, space and energy compatibility allows to reconstruct the incident direction of the prompt  $\gamma$ , within a probability cone. The lower energy annihilation photons are detected in the absorber layer and define the line of response. The annihilation is located at the point(s) where the Compton cone intersects the line of response. While some detectors rely on separate scattering and absorber layers such as in [106] or [145], others rely on their ability to reconstruct multiple Compton interactions within the same layer and do not require a scattering and absorbing layer such as [143].

The prompt gamma is used to provide the  $\beta^+$  decay time and serve as a marker of positron emission. The detection of the annihilation photons then marks the annihilation of the positron, either through a direct annihilation or after transiting through a positronium state. This measurement would permit to measure the lifetime of positrons in the body. However, in most iterative PET image reconstruction algorithms, the final reconstructed radiotracer distribution is an ersatz distribution that would produce a collection of line of responses compatible with the observed collection of line of response actually observed. Information on an event-by-event basis is lost. This makes it impossible to propagate the time

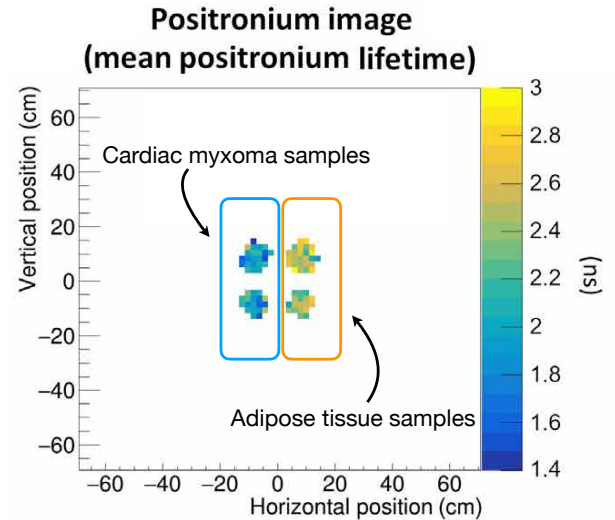


Fig. 8. First positronium lifetime image from the J-PET research group, modified and annotated from [106], under Creative Commons Attribution License 4.0 (CC BY).

delays of individual coincidences to a given voxel in the final image volume. Simple reconstructions such as filtered back projection can be modified to distribute the time delay of each events along their line of response but are sub-optimal in terms of spatial resolution of the reconstructed image. This reconstruction technique was employed for the proof of concept of positronium imaging performed by the J-PET research group [106] which produced the first positronium lifetime image, in figure 8, of four samples in the field of view of the J-PET tomograph : two cardiac myxoma and two adipose tissue samples. To produce this image, each sample was placed in a holder along with a  $^{22}\text{Na}$  source ranging from  $\sim 0.2$  to  $\sim 0.4$  MBq, which produced the prompt  $\gamma$  at the moment of annihilation and irradiated the samples with positrons. For each voxel in the image, the mean value of the distribution of the time delays is reported. As the lifetime for direct annihilation and  $p\text{-Ps}$  are not dependent of the medium, and are much smaller than the time resolution of the tomograph, the mean lifetime is strongly correlated to the lifetime of  $o\text{-Ps}$ , and provides information on the annihilation medium.

Positrons in figure 8 were produced by a  $^{22}\text{Na}$  source directly in contact with the samples, however, in order to perform *in vivo* positronium imaging,  $(\beta^+, \gamma)$  isotopes must reach the regions of interest in the body. Therefore this imaging requires a radiotracer similar to what is traditionally used in PET. Among the several  $(\beta^+, \gamma)$  radioisotopes considered,  $^{44g}\text{Sc}$  seems the best candidate with a lifetime realistically suited to perform molecular imaging [118], [129], and already studied associated pharmaceuticals and biodistributions [119]–[128]. However, none of these pharmaceuticals are used in clinical practice yet.

The positronium information will be an additional layer from the uneven tracer distribution, often expressed as the standard uptake value (SUV), i.e. the relative local concentration of

tracer compared to the averaged tracer concentration in the full body. A region with higher SUV means a higher concentration of the expression of the biological function targeted by the tracer, hence a higher probability of anomalous cells in that region. This region will also provide a higher statistical measurement for positronium lifetime. A comparison of  $\tau_{\text{oPs}}$  between healthy and pathological regions of a same organ will therefore suffer from this large difference of statistics when evaluating the various  $\tau_{\text{oPs}}$  values. However, positronium imaging in PET will add a layer of information to the simple SUV, enabling medical diagnostic to hopefully detect physical and chemical changes in tissues before their impact on the biological functions manifest into a radiotracer uptake change [22].

In the wake of developing PET prototypes able to perform positronium imaging, and the growing interest of this imaging modality in the field, reconstruction algorithms are being developed to recover higher spatial resolution in the final image than filtered back projection algorithms, while propagating the time delay distributions to each individual voxel. Likelihood maximization algorithms associated to multiple lifetime fitting are being developed [146], [147]. [148] reaches a 4 mm spatial resolution on 2D simulated phantoms. [149] studied the impact of the coincidence time resolution (CTR) of tomographs on the ability to reach high spatial and temporal resolution. The CTR has two impacts on the final positronium lifetime image : it introduces spatial blurring in the image, making it harder to distinguish neighbouring regions of separated positronium lifetimes, and it introduces an error on the measured lifetime, preventing separation of regions with lifetime differences small compared to the CTR (i.e. a CTR of 500 ps and a lifetime difference of 0.2 ns).

The SPLIT algorithm [150] proposes a statistical lifetime reconstruction by reconstructing consecutive activity images with a progressively increasing coincidence window between the prompt  $\gamma$  and the annihilation photons. This algorithm was shown to perform similarly to a likelihood maximization algorithm such as [151] and [152], while keeping a better stability in lifetime measurement when positronium sources are close to each other. In addition to Monte-Carlo simulations, the SPLIT algorithm has been successfully applied to actual J-PET ex-vivo data.

At the time of this review, while the first *in-vivo* positronium image of the brain has been presented using  $^{68}\text{Ga}$ -PSMA as radiotracer [27], [28], no definitive use of positronium imaging to medical diagnosis has been proposed, since a change in positronium lifetime means a change in free volumes in tissue, which can have many underlying causes. However the development of tools to study the behaviour of  $\tau_{\text{oPs}}$  in vivo may procure a way to better understand this parameter and find use cases not yet foreseen. The important variability from subject to subject of  $\tau_{\text{oPs}}$  for similar healthy tissue, preventing to establish a reference atlas, is an additional limitation, but can be mitigated by the comparison, when possible, for a same patient of  $\tau_{\text{oPs}}$  from a healthy part of a tissue to its pathological region.

## VIII. CONCLUSION

Positron annihilation lifetime spectroscopy is widely used in materials science to study the structure of materials at the atomic level. The application of PALS in life sciences is still in its early stage. Natural tissues and organs are highly complex systems with the chemical compositions and physical structures that can vary significantly from sample to sample, variables to which PALS is highly sensitive. Moreover, the interpretation of PALS results require very well characterized, controlled, and systematic samples. Studies have been performed to correlate the positron lifetime in *ex vivo* biological samples to various parameters, including oxygen saturation in tissues, temperature, or presence of lead. Knowing the parameter being varied, PALS is a good tool to follow its evolution, but linking a change in positronium lifetime to a single parameter is not yet understood. The best approach in this application is to pursue interdisciplinary investigations in a joint effort among physical, chemical, biological, and medical scientists.

Thanks to the development of high sensitivity full body PET with improving time resolution, the possibility to use *in vivo* positronium events as a way to extract information on the surrounding tissue from the positron annihilation itself has been proposed. A proof of concept has been performed by the J-PET research group who produced the first voxelized image of the positronium mean lifetime in four biological samples.

Limits to spatial and temporal resolutions of the images are mostly linked to the temporal resolution of the apparatus and the activity per voxel. Moreover, the uncertain correlation of a change in  $\tau_{\text{oPs}}$  to a given pathology, and the important variability, for a given tissue, from one subject to another are obstacles that will need to be overcome before positronium lifetime imaging can be used in a medical setting.

The future high sensitivity full body  $3\gamma$ -capable PET will provide a powerful mean of measuring  $\tau_{\text{oPs}}$  *in-vivo*, overcoming these first two limitations. This will allow biologists to perform high resolution studies on larger sample sizes, hopefully highlighting correlations to pathologies, and making  $\tau_{\text{oPs}}$  imaging a promising tool for future clinical diagnostics.

## ACKNOWLEDGEMENTS

All authors declare that they have no known conflicts of interest in terms of competing financial interests or personal relationships that could have an influence or are relevant to the work reported in this paper.

## REFERENCES

- [1] Abass Alavi, Thomas J Werner, Ewa L Stepień, and Paweł Moskal. Unparalleled and revolutionary impact of pet imaging on research and day to day practice of medicine. *Bio-Algorithms and Med-Systems*, 17(4):203–212, 2021.

- [2] M.A. Pysz, S.S. Gambhir, and J.K. Willmann. Molecular imaging: current status and emerging strategies. *Clinical radiology*, 65(7):500–516, 2010.
- [3] Jingli Wang and Laura Maurer. Positron emission tomography: applications in drug discovery and drug development. *Current topics in medicinal chemistry*, 5(11):1053–1075, 2005.
- [4] Jurgen K. Willmann, Nicholas van Bruggen, Ludger M. Dinkelborg, and Sanjiv S. Gambhir. Molecular imaging in drug development. *Nature Reviews Drug Discovery*, 7(7):591–607, 2008.
- [5] Heinz H Coenen and Johannes Ermert. Expanding pet-applications in life sciences with positron-emitters beyond fluorine-18. *Nuclear medicine and biology*, 92:241–269, 2021.
- [6] Aadne Ore and JL Powell. Three-photon annihilation of an electron-positron pair. *Physical Review*, 75(11):1696, 1949.
- [7] Stephan Berko and Hugh N Pendleton. Positronium. *Annual Review of Nuclear and Particle Science*, 30(1):543–581, 1980.
- [8] Sergey V Stepanov, Vsevolod M Byakov, and Tetsuya Hirade. To the theory of ps formation and Johannes Ermert. Expanding pet-applications in life sciences with positron-emitters beyond fluorine-18. *Radiation Physics and Chemistry*, 76(2):90–95, 2007.
- [9] PS Stepanov, FA Selim, SV Stepanov, AV Bokov, OV Ilyukhina, G Duplâtre, and VM Byakov. Interaction of positronium with dissolved oxygen in liquids. *Physical Chemistry Chemical Physics*, 22(9):5123–5131, 2020.
- [10] GS Adkins, DB Cassidy, and J Pérez-Ríos. Precision spectroscopy of positronium: Testing bound-state qed theory and the search for physics beyond the standard model. *Physics Reports*, 975:1–61, 2022.
- [11] NG Chechenin, A Van Veen, R Escobar Galindo, H Schut, AR Chezan, PM Bronsveld, J Th M De Hosson, and DO Boerma. Positron annihilation and transmission electron microscopy study of the evolution of microstructure in cold-rolled and nitrided ferri foils. *Journal of Physics: Condensed Matter*, 13(26):5937, 2001.
- [12] Yawei Zhou, Wenfeng Mao, Qichao Li, Juncheng Wang, and Chunqing He. Formation and annihilation of positronium in silica aerogels under atmosphere of oxygen and nitrogen mixture. *Chemical Physics*, 459:81–86, 2015.
- [13] Sergey V Stepanov, Vsevolod M Byakov, Dmitrii S Zvezhinskiy, Gilles Duplâtre, Roman R Nurmukhametov, and Petr S Stepanov. Positronium in a liquid phase: Formation, bubble state and chemical reactions. *Advances in Physical Chemistry*, 2012, 2012.
- [14] MA Alkhorayef, EI Abuelhia, MPW Chin, and NM Spyrou. Determination of the relative oxygenation of samples by ortho-positronium 3-gamma decay for future application in oncology. *Journal of radio-analytical and nuclear chemistry*, 281:171–174, 2009.
- [15] Kengo Shibuya, Haruo Saito, Fumihiko Nishikido, Miwako Takahashi, and Taiga Yamaya. Oxygen sensing ability of positronium atom for tumor hypoxia imaging. *Communications Physics*, 3(1):173, 2020.
- [16] Pawel Moskal and Ewa L Stepien. Positronium as a biomarker of hypoxia. *Bio-Algorithms and Med-Systems*, 17(4):311–319, 2021.
- [17] Eneko Axpe, Tamara Lopez-Euba, Ainara Castellanos-Rubio, David Merida, Jose Angel Garcia, Leticia Plaza-Izurietta, Nora Fernandez-Jimenez, Fernando Plazaola, and Jose Ramon Bilbao. Detection of atomic scale changes in the free volume void size of three-dimensional colorectal cancer cell culture using positron annihilation lifetime spectroscopy. *PLoS One*, 9(1):e83838, 2014.
- [18] Pawel Moskal, Ewelina Kubicz, Grzegorz Grudzien, Eryk Czerwinski, Kamil Dulski, Bartosz Leszczynski, Szymon Niedzwiecki, and Ewa L Stepien. Developing a novel positronium biomarker for cardiac myxoma imaging. *EJNMMI physics*, 10(1):22, 2023.
- [19] Simbarashe Moyo, Pawel Moskal, and Ewa Stepien. Feasibility study of positronium application for blood clots structural characteristics. *Bio-Algorithms and Med-Systems*, 18(1):163–167, 2022.
- [20] Steven D Bass, Sebastiano Mariazzi, Pawel Moskal, and Ewa Stepien. Colloquium: Positronium physics and biomedical applications. *Reviews of Modern Physics*, 95(2):021002, 2023.
- [21] Pawel Moskal. Towards total-body modular pet for positronium and quantum entanglement imaging. In *2018 IEEE Nuclear Science Symposium and Medical Imaging Conference Proceedings (NSS/MIC)*, pages 1–4. IEEE, 2018.
- [22] Pawel Moskal, Bożena Jasińska, Ewa Ł Stepień, and Steven D Bass. Positronium in medicine and biology. *Nature Reviews Physics*, 1(9):527–529, 2019.
- [23] Pawel Moskal. Positronium imaging. In *2019 IEEE nuclear science symposium and medical imaging conference (NSS/MIC)*, pages 1–3. IEEE, 2019.
- [24] Mateusz Sitarz, Jean-Pierre Cussonneau, Tomasz Matulewicz, and Ferid Haddad. Radionuclide candidates for  $\beta^+$   $\gamma$  coincidence pet: an overview. *Applied Radiation and Isotopes*, 155:108898, 2020.
- [25] Tomasz Matulewicz. Radioactive nuclei for  $\beta^+$   $\gamma$  pet and theranostics: selected candidates. *Bio-Algorithms and Med-Systems*, 17(4):235–239, 2021.
- [26] Manish Das, Wiktor Mryka, Ermias Yitayew Beyene, Szymon Parzych, Sushil Sharma, Ewa Stepien, and Pawel Moskal. Estimating the efficiency and purity for detecting annihilation and prompt photons for positronium imaging with j-pet using toy monte carlo simulation. *Bio-Algorithms and Med-Systems*, 19(1):87–95, 2023.
- [27] P. Moskal et al. The first in-vivo positronium imaging of the human brain. In *2022 IEEE Nuclear Science Symposium, Medical Imaging Conference and Room Temperature Semiconductor Measurements*, Milano, Italy, November 5-12 2022.
- [28] Pawel Moskal, Jakub Baran, Steven Bass, Jaroslaw Choinski, Neha Chug, Catalina Curceanu, Eryk Czerwinski, Meysam Dadgar, Manish Das, Kamil L Dulski, et al. First positronium image of the human brain in vivo. *medRxiv*, pages 2024–02, 2024.
- [29] J. Pirenne. *PhD Thesis : Le champ propre et l'interaction des particules de Dirac : suivant l'électrodynamique quantique*. PhD thesis, University of Paris, 1944. Arch. Sci Phys. Nat.28 (1946) 233.
- [30] J. Pirenne. *PhD Thesis : Le champ propre et l'interaction des particules de Dirac : suivant l'électrodynamique quantique [suite]*. PhD thesis, University of Paris, 1944. Arch. Sci Phys. Nat. 29:121; 29:207, 29:265.
- [31] John Archibald Wheeler. Polyelectrons. *Annals of the New York Academy of Sciences*, 48(3):219–238, 1946.
- [32] Martin Deutsch. Evidence for the formation of positronium in gases. *Physical Review*, 82(3):455, 1951.
- [33] Martin Deutsch. Three-quantum decay of positronium. *Physical Review*, 83(4):866, 1951.
- [34] Martin Deutsch and Everett Dulit. Short range interaction of electrons and fine structure of positronium. *Physical Review*, 84(3):601, 1951.
- [35] T Yamazaki, A Miyazaki, T Suehara, T Namba, S Asai, T Kobayashi, H Saito, I Ogawa, T Idehara, and S Sabchevski. Direct observation of the hyperfine transition of ground-state positronium. *Physical review letters*, 108(25):253401, 2012.
- [36] LR Kasday, JD Ullman, and CS Wu. Angular correlation of compton-scattered annihilation photons and hidden variables. *Il Nuovo Cimento B (1971-1996)*, 25(2):633–661, 1975.
- [37] Pawel Moskal, Eryk Czerwiński, Juhı Raj, Steven D Bass, Ermias Y Beyene, Neha Chug, Aurélien Coussat, Catalina Curceanu, Meysam Dadgar, Manish Das, et al. Discrete symmetries tested at 10- 4 precision using linear polarization of photons from positronium annihilations. *Nature Communications*, 15(1):78, 2024.
- [38] S DeBenedetti and HC Corben. Positronium. *Annual Review of Nuclear Science*, 4(1):191–218, 1954.
- [39] S. D. Bass. Qed and fundamental symmetries in positronium decays. *Acta Physica Polonica. B*, 50(1319), 2019.
- [40] ED Theriot Jr, RH Beers, and VW Hughes. Precision redetermination of the hyperfine structure interval of positronium. *Physical Review Letters*, 18(19):767, 1967.
- [41] RH Beers and VW Hughes. Annihilation rate of orthopositronium. In *BULLETIN OF THE AMERICAN PHYSICAL SOCIETY*, volume 13 4, page 633. AMER INST PHYSICS CIRCULATION FULFILLMENT DIV, 500 SUNNYSIDE BLVD, WOODBURY ..., 1968.
- [42] PG Coleman and TC Griffith. An accurate measurement of the natural decay rate of orthopositronium. *Journal of Physics B: Atomic and Molecular Physics*, 6(10):2155, 1973.
- [43] S Asai, S Orito, and N Shinohara. New measurement of the orthopositronium decay rate. *Physics Letters B*, 357(3):475–480, 1995.
- [44] Richard Ley and Gunter Werth. *Positronium: Theory Versus Experiment*, pages 407–418. Springer Berlin Heidelberg, Berlin, Heidelberg, 2001.
- [45] Richard Sterling Vallery, PW Zitzewitz, and DW Gidley. Resolution of the orthopositronium-lifetime puzzle. *Physical review letters*, 90(20):203402, 2003.
- [46] AH Al-Ramadhan and DW Gidley. New precision measurement of the decay rate of singlet positronium. *Physical Review Letters*, 72(11):1632, 1994.
- [47] Y Kataoka, S Asai, and T Kobayashi. First test of order ( $\alpha^2$ ) correction of the orthopositronium decay rate. *Physics Letters B*, 671(2):219–223, 2009.
- [48] David W Gidley, Kenneth A Marko, and Arthur Rich. Precision measurement of the decay rate of orthopositronium in sio<sub>2</sub> powders. *Physical Review Letters*, 36(8):395, 1976.
- [49] DW Gidley, PW Zitzewitz, KA Marko, and A Rich. Measurement of the vacuum decay rate of orthopositronium. *Physical Review Letters*, 37(12):729, 1976.

- [50] DW Gidley, A Rich, PW Zitzewitz, and DAL Paul. New experimental value for the orthopositronium decay rate. *Physical Review Letters*, 40(12):737, 1978.
- [51] TC Griffith, GR Heyland, KS Lines, and TR Twomey. The decay rate of ortho-positronium in vacuum. *Journal of Physics B: Atomic and Molecular Physics*, 11(23):L743, 1978.
- [52] DW Gidley, A Rich, E Sweetman, and D West. New precision measurements of the decay rates of singlet and triplet positronium. *Physical Review Letters*, 49(8):525, 1982.
- [53] CI Westbrook, DW Gidley, RS Conti, and A Rich. New precision measurement of the orthopositronium decay rate: a discrepancy with theory. *Physical Review Letters*, 58(13):1328, 1987.
- [54] Jeffrey Scott Nico, DW Gidley, A Rich, and PW Zitzewitz. Precision measurement of the orthopositronium decay rate using the vacuum technique. *Physical Review Letters*, 65(11):1344, 1990.
- [55] Osamu Jinnouchi, S Asai, and T Kobayashi. Precision measurement of orthopositronium decay rate using sio2 powder. *Physics Letters B*, 572(3-4):117–126, 2003.
- [56] A Ore. Annihilation of positrons in gases, årbok/universitetet i bergen. *Naturvitenskapelig rekke*, 9, 1949.
- [57] O-E\_ Mogensen. Spur reaction model of positronium formation. *The Journal of Chemical Physics*, 60(3):998–1004, 1974.
- [58] Roy Neil West. Positron studies of condensed matter. *Advances in Physics*, 22(3):263–383, 1973.
- [59] M. Doyama. Proceedings of the fifth international conference on positron annihilation, april 8-11, 1979, lake yamanaka, japan. In *Sendai, Japan: The Japan Institute of Metals*, pages 13–30, 1979.
- [60] Richard A Ferrell. Long lifetime of positronium in liquid helium. *Physical Review*, 108(2):167, 1957.
- [61] SJ Tao. Positronium annihilation in molecular substances. *The Journal of Chemical Physics*, 56(11):5499–5510, 1972.
- [62] Morten Eldrup, D Lightbody, and John Neil Sherwood. The temperature dependence of positron lifetimes in solid pivalic acid. *Chemical Physics*, 63(1-2):51–58, 1981.
- [63] H Nakanishi. Microscopic surface tension studied by positron annihilation. In *Int. Symp. on Positron Annihilation Studies of Fluids*, pages 292–298. World Scientific, 1988.
- [64] A Uedono, N Inoue, Y Hayashi, K Eguchi, T Nakamura, Y Hirose, M Yoshimaru, N Oshima, T Ohdaira, and R Suzuki. Damage characterization of low-k layers through cu damascene process using monoenergetic positron beams. In *2010 IEEE International Interconnect Technology Conference*, pages 1–3. IEEE, 2010.
- [65] A Biganeh, O Kakuee, H Rafi-Kheiri, M Lamehi-Rachti, N Sheikh, and E Yahaghi. Positron annihilation lifetime and doppler broadening spectroscopy of polymers. *Radiation Physics and Chemistry*, 166:108461, 2020.
- [66] S Berko. Electrons in disordered metals and at metallic surfaces ed p phariseau, bl gyorffy and l scheire. *New York: Plenum*, 1(1):221–53, 1979.
- [67] PE Mijnders. Positrons in solids ed p hautojärvi, 1979.
- [68] Y C Jean. Positron annihilation spectroscopy for chemical analysis: a novel probe for microstructural analysis of polymers. *Microchemical Journal*, 42(1):72–102, 1990.
- [69] RK Wilson, PO Johnson, and R Stump. Variation in positron lifetime with pressure. *Physical Review*, 129(5):2091, 1963.
- [70] Tomasz Goworek. Positronium as a probe of small free volumes in crystals, polymers and porous media. *Annales Universitatis Mariae Curie-Skłodowska, sectio AA—Chemia*, 69(1-2):1, 2015.
- [71] Vladimir Slugen, Jarmila Degmova, Stanislav Sojak, Martin Petriska, Pavol Noga, and Vladimir Krsjak. On the limitations of positron annihilation spectroscopy in the investigation of ion-implanted fecr samples. *Metals*, 11(11):1689, 2021.
- [72] I Mincov, MP Petkov, P Tsou, and T Troev. Porosity characterization of aerogels using positron annihilation lifetime spectroscopy. *Journal of non-crystalline solids*, 350:253–258, 2004.
- [73] Charlene J Edvardson, Michael DW Grogan, Timothy A Birks, and Paul G Coleman. Positron and positronium studies of silica aerogel. In *Journal of Physics: Conference Series*, volume 262 1, page 012018. IOP Publishing, 2011.
- [74] Chunqing He, Shaojie Wang, Yoshinori Kobayashi, Toshiyuki Ohdaira, and Ryoichi Suzuki. Role of pore morphology in positronium diffusion in mesoporous silica thin films and in positronium emission from the surfaces. *Physical Review B*, 86(7):075415, 2012.
- [75] Halyna Klym, Ivan Karbovnyk, Sergei Piskunov, and Anatoli I Popov. Positron annihilation lifetime spectroscopy insight on free volume conversion of nanostructured mgal2o4 ceramics. *Nanomaterials*, 11(12):3373, 2021.
- [76] Petra Castellaz, Andreas Siegle, and Hermann Stoll. Positron age-momentum-correlation (amoc) measurements on organic liquids. *Journal of Nuclear and Radiochemical Sciences*, 3(2):R1–R7, 2002.
- [77] Chunqing He, Takenori Suzuki, VP Shantarovich, Kenjiro Kondo, and Yasuo Ito. Positron annihilation in hypercrosslinked polystyrenes. *Chemical physics*, 286(2-3):249–256, 2003.
- [78] Celesta Fong, Aurelia W Dong, Anita J Hill, Ben J Boyd, and Calum J Drummond. Positron annihilation lifetime spectroscopy (pals): a probe for molecular organisation in self-assembled biomimetic systems. *Physical Chemistry Chemical Physics*, 17(27):17527–17540, 2015.
- [79] M Leventhal, CJ MacCallum, and PD Stang. Detection of 511 keV positron annihilation radiation from the galactic center direction. *Gamma Ray Spectroscopy In Astrophysics*, page 169, 1978.
- [80] Davide Franco, Giovanni Consolati, and D Trezzi. Positronium signature in organic liquid scintillators for neutrino experiments. *Physical Review C*, 83(1):015504, 2011.
- [81] S Perasso, GIOVANNI Consolati, D Franco, C Jollet, A Mereaglia, A Tonazzo, and M Yeh. Measurement of ortho-positronium properties in liquid scintillators. *Journal of Instrumentation*, 9(03):C03028, 2014.
- [82] Y Abe, JC Dos Anjos, JC Barriere, E Baussan, I Bekman, M Bergevin, TJC Bezerra, L Bezrukov, E Blucher, C Buck, et al. Ortho-positronium observation in the double chooz experiment. *Journal of High Energy Physics*, 2014(10):1–17, 2014.
- [83] Mario Schwarz, Sabrina M Franke, Lothar Oberauer, Miriam D Plein, Hans Th J Steiger, and Marc Tippmann. Measurements of the lifetime of orthopositronium in the lab-based liquid scintillator of juno. *Nuclear Instruments and Methods in Physics Research Section A: Accelerators, Spectrometers, Detectors and Associated Equipment*, 922:64–70, 2019.
- [84] Gianpaolo Bellini, J Benziger, D Bick, S Bonetti, G Bonfini, D Bravo, M Buizza Avanzini, B Caccianiga, L Cadonati, F Calaprice, et al. First evidence of p e p solar neutrinos by direct detection in borexino. *Physical Review Letters*, 108(5):051302, 2012.
- [85] Petri Sane, Emppu Salonen, Emma Falck, Jarmila Repakova, Filip Tuomisto, Juha M Holopainen, and Ilpo Vattulainen. Probing biomembranes with positrons. *The Journal of Physical Chemistry B*, 113(7):1810–1812, 2009.
- [86] S Siles, G Moya, X Li, J Kansy, and P Moser. Positron annihilation lifetime measurements in collagen biopolymer. *Journal of radioanalytical and nuclear chemistry*, 240(2):529–530, 1999.
- [87] Petri Sane, Filip Tuomisto, Susanne K Wiedmer, Tuula Nyman, Ilpo Vattulainen, and Juha M Holopainen. Temperature-induced structural transition in-situ in porcine lens—changes observed in void size distribution. *Biochimica et Biophysica Acta (BBA)-Biomembranes*, 1798(5):958–965, 2010.
- [88] SH Yang, C Ballmann, and CA Quarles. Positron spectroscopy investigation of normal brain section and brain section with glioma derived from a rat glioma model. In *AIP Conference Proceedings*, volume 1099 1, pages 948–951. American Institute of Physics, 2009.
- [89] Guang Liu, Hongmin Chen, Lakshmi Chakka, Joseph E Gadzia, and YC Jean. Applications of positron annihilation to dermatology and skin cancer. *physica status solidi c*, 4(10):3912–3915, 2007.
- [90] Guang Liu, Hongmin Chen, Lakshmi Chakka, Mei-Ling Cheng, Joseph E Gadzia, R Suzuki, T Ohdaira, N Oshima, and YC Jean. Further search for selectivity of positron annihilation in the skin and cancerous systems. *Applied surface science*, 255(1):115–118, 2008.
- [91] YC Jean, Ying Li, Gaung Liu, Hongmin Chen, Junjie Zhang, and Joseph E Gadzia. Applications of slow positrons to cancer research: Search for selectivity of positron annihilation to skin cancer. *Applied surface science*, 252(9):3166–3171, 2006.
- [92] YC Jean, Hongmin Chen, Guang Liu, and Joseph E Gadzia. Life science research using positron annihilation spectroscopy: Uv-irradiated mouse skin. *Radiation Physics and Chemistry*, 76(2):70–75, 2007.
- [93] Ting Lu. The change in microstructure of plant seeds induced by low energy ion implantation. *Wuli*, 31(9):555–557, 2002.
- [94] T Lu. A study of mechanism of biological effect on plants caused by ion implantation. *Looking to the 21st century. World Scientific Publishing Co, Singapore*, 1997.
- [95] Gaëlle Roudaut and G Duplâtre. Positronium as a probe in natural polymers: decomposition in starch. *Physical Chemistry Chemical Physics*, 11(41):9556–9561, 2009.
- [96] MA Ali, HF Mohamed, and WM Amer. Biophysical measurements of lead in some bioindicator plants. *Rom. J. Biophys.*, 18(1):57–66, 2008.
- [97] Hong Min Chen, J David Van Horn, and Yan Ching Jean. Applications of positron annihilation spectroscopy to life science. In *Defect and diffusion forum*, volume 331, pages 275–293. Trans Tech Publ, 2012.

- [98] FH Hsu, BG Wen, JFR Kuck, and NT Yu. Positron annihilation studies of age-induced changes in animal lenses. *physica status solidi (a)*, 102(2):571–575, 1987.
- [99] DR Gustafson. Positronium formation in muscle: an investigation of the structure of cell water. *Biophysical Journal*, 10(4):316–322, 1970.
- [100] Hanieh Karimi, Pawel Moskal, Agata Zak, and Ewa L Stepień. 3d melanoma spheroid model for the development of positronium biomarkers. *Scientific Reports*, 13(1):7648, 2023.
- [101] DeonJ Venter, Sanjeev Kumar, NadiaL Tuzi, and WilliamJ Gullick. Overexpression of the c-erbB-2 oncoprotein in human breast carcinomas: immunohistological assessment correlates with gene amplification. *The Lancet*, 330(8550):69–72, 1987.
- [102] I Rubin and Yosef Yarden. The basic biology of her2. *Annals of oncology*, 12:S3–S8, 2001.
- [103] Hadis Honarvar, Cristina Müller, Susan Cohrs, Stephanie Haller, Kristina Westerlund, Amelie Eriksson Karlström, Nicholas P van der Meulen, Roger Schibli, and Vladimir Tolmachev. Evaluation of the first 44sc-labeled affibody molecule for imaging of her2-expressing tumors. *Nuclear medicine and biology*, 45:15–21, 2017.
- [104] Chuanyuan Yin, Donglin Guo, Tao Xi, Xianxiu Xu, and Qingchao Gu. Studies on structural features of human tumor necrosis factor. *Nuclear Science and Techniques*, 8(4):218–220, 1997.
- [105] B Jasińska, B Zgardzińska, G Cholibek, M Pietrow, M Gorgol, K Wiktor, K Wysoglad, Piotr Białas, C Curceanu, Eryk Czerwiński, et al. Human tissue investigations using pals technique: free radicals influence. *Acta Physica Polonica. A*, 132(5), 2017.
- [106] Pawel Moskal, Kamil Dulski, Neha Chug, Catalina Curceanu, Eryk Czerwiński, Meysam Dadgar, Jan Gajewski, Aleksander Gajos, Grzegorz Grudzień, Beatrix C Hiesmayr, et al. Positronium imaging with the novel multiphoton pet scanner. *Science advances*, 7(42):eabh4394, 2021.
- [107] MN Chandrashekhara and C Ranganathaiah. Chemical and photochemical degradation of human hair: A free-volume microprobe study. *Journal of Photochemistry and Photobiology B: Biology*, 101(3):286–294, 2010.
- [108] MN Chandrashekhara and C Ranganathaiah. Diffusion of permanent liquid dye molecules in human hair investigated by positron lifetime spectroscopy. *Colloids and Surfaces B: Biointerfaces*, 69(1):129–134, 2009.
- [109] Yoshiaki Itoh, Akira Shimazu, Yasuyuki Sadzuka, Takashi Sonobe, and Shigeru Itai. Novel method for stratum corneum pore size determination using positron annihilation lifetime spectroscopy. *International journal of pharmaceuticals*, 358(1-2):91–95, 2008.
- [110] K. Kacperski, N.M. Spyrou, and F.A. Smith. Three-gamma annihilation imaging in positron emission tomography. *IEEE Transactions on Medical Imaging*, 23(4):525–529, 2004.
- [111] Krzysztof Kacperski and Nicholas M Spyrou. Performance of three-photon pet imaging: Monte carlo simulations. *Physics in Medicine & Biology*, 50(23):5679, nov 2005.
- [112] Changyeon Yoon, Wonho Lee, and Taewoong Lee. Simulation for czt compton pet (maximization of the efficiency for pet using compton event). *Nuclear Instruments and Methods in Physics Research Section A: Accelerators, Spectrometers, Detectors and Associated Equipment*, 652(1):713–716, 2011.
- [113] Y Gu, JL Matteson, RT Skelton, AC Deal, EA Stephan, F Duttweiler, TM Gasaway, and CS Levin. Study of a high-resolution, 3d positioning cadmium zinc telluride detector for pet. *Physics in Medicine & Biology*, 56(6):1563, 2011.
- [114] Shiva Abbaszadeh, Garry Chinn, and Craig S Levin. Positioning true coincidences that undergo inter-and intra-crystal scatter for a sub-mm resolution cadmium zinc telluride-based pet system. *Physics in Medicine & Biology*, 63(2):025012, 2018.
- [115] Aleksander Gajos, D Kamińska, Eryk Czerwiński, Dominika Alfs, Tomasz Bednarski, Piotr Białas, Bartosz Głowacz, M Gorgol, B Jasińska, G Korcyl, et al. Trilateration-based reconstruction of ortho-positronium decays into three photons with the j-pet detector. *Nuclear Instruments and Methods in Physics Research Section A: Accelerators, Spectrometers, Detectors and Associated Equipment*, 819:54–59, 2016.
- [116] Pawel Moskal, Aleksander Gajos, Muhsin Mohammed, Jyoti Chhokar, Neha Chug, Catalina Curceanu, Eryk Czerwiński, Meysam Dadgar, Kamil Dulski, Marek Gorgol, et al. Testing cpt symmetry in ortho-positronium decays with positronium annihilation tomography. *Nature communications*, 12(1):5658, 2021.
- [117] Paul Lecoq, Christian Morel, John O Prior, Dimitris Visvikis, Stefan Gundacker, Etienne Auffray, Peter Krizan, Rosana Martinez Turtos, Dominique Thers, Edoardo Charbon, et al. Roadmap toward the 10 ps time-of-flight pet challenge. *Physics in Medicine & Biology*, 65(21):21RM01, 2020.
- [118] P Thirof, C Lang, and K Parodi. Perspectives for highly-sensitive pet-based medical imaging using  $\beta^+ \gamma$  coincidences. *Acta Physica Polonica A*, 127(5):1441–1444, 2015.
- [119] Sandrine Huclier-Markai, Cyrille Alliot, Rabha Kerdjoudj, Marie Mougin-Degraef, Nicolas Chouin, and Ferid Haddad. Promising scandium radionuclides for nuclear medicine: a review on the production and chemistry up to in vivo proofs of concept. *Cancer biotherapy & radiopharmaceuticals*, 33(8):316–329, 2018.
- [120] Eftychia Koumariou, Dariusz Pawlak, Agnieszka Korsak, and Renata Mikolajczak. Comparison of receptor affinity of nat sc-dota-tate versus nat ga-dota-tate. *Nuclear Medicine Review*, 14(2):85–89, 2011.
- [121] Seweryn Krajewski, Izabela Cydzik, Kamel Abbas, Antonio Bulgheroni, Aleksander Bilewicz, Agnieszka Majkowska-Pilip, and Federica Simonell. Labelling of dotatate with cyclotron produced 44sc. *Prof. Jacek Michalik, Ph. D., D. Sc. Wiktor Smutek, Ph. D.*, page 42, 2012.
- [122] Marek Pruszyński, Agnieszka Majkowska-Pilip, Natalia S Loktionova, Elisabeth Eppard, and Frank Roesch. Radiolabeling of dotatoc with the long-lived positron emitter 44sc. *Applied Radiation and Isotopes*, 70(6):974–979, 2012.
- [123] F Roesch. Scandium-44: benefits of a long-lived pet radionuclide available from the 44ti/44sc generator system. *Current radiopharmaceuticals*, 5(3):187–201, 2012.
- [124] Cristina Müller, Maruta Bunka, Josefine Reber, Cindy Fischer, Konstantin Zhernosekov, Andreas Türler, and Roger Schibli. Promises of cyclotron-produced 44sc as a diagnostic match for trivalent  $\beta^-$ -emitters: in vitro and in vivo study of a 44sc-dota-folate conjugate. *Journal of nuclear medicine*, 54(12):2168–2174, 2013.
- [125] S Huclier-Markai, R Kerdjoudj, C Alliot, AC Bonraisin, N Michel, F Haddad, and J Barbet. Optimization of reaction conditions for the radiolabeling of dota and dota-peptide with 44m/44sc and experimental evidence of the feasibility of an in vivo pet generator. *Nuclear medicine and biology*, 41:e36–e43, 2014.
- [126] Nicholas P van der Meulen, Maruta Bunka, Katharina A Domnanich, Cristina Müller, Stephanie Haller, Christiaan Vermeulen, Andreas Türler, and Roger Schibli. Cyclotron production of 44sc: from bench to bedside. *Nuclear medicine and biology*, 42(9):745–751, 2015.
- [127] Katharina A Domnanich, Cristina Müller, Renata Farkas, Raffaella M Schmid, Bernard Ponsard, Roger Schibli, Andreas Türler, and Nicholas P van der Meulen. 44sc for labeling of dota-and nodaga-functionalized peptides: preclinical in vitro and in vivo investigations. *EJNMMI Radiopharmacy and Chemistry*, 1(1):1–19, 2017.
- [128] Krzysztof Kilian, Lukasz Cheda, Mateusz Sitarz, Katarzyna Szkliniarz, Jaroslaw Choinski, and Anna Stolarz. Separation of 44sc from natural calcium carbonate targets for synthesis of 44sc-dotatate. *Molecules*, 23(7):1787, 2018.
- [129] Pawel Moskal and Ewa Stepień. Prospects and clinical perspectives of total-body pet imaging using plastic scintillators. *PET clinics*, 15(4):439–452, 2020.
- [130] Simon R Cherry, Johanna Diekmann, and Frank M Bengel. Total-body positron emission tomography. *JACC: CARDIOVASCULAR IMAGING*, 16(10), 2023.
- [131] Ramsey D Badawi, Hongcheng Shi, Pengcheng Hu, Shuguang Chen, Tianyi Xu, Patricia M Price, Yu Ding, Benjamin A Spencer, Lorenzo Nardo, Weiping Liu, et al. First human imaging studies with the explorer total-body pet scanner. *Journal of Nuclear Medicine*, 60(3):299–303, 2019.
- [132] Austin R Pantel, Varsha Viswanath, Margaret E Daube-Witherspoon, Jacob G Dubroff, Gerd Muehllehner, Michael J Parma, Daniel A Pryma, Erin K Schubert, David A Mankoff, and Joel S Karp. Pennpet explorer: human imaging on a whole-body imager. *Journal of Nuclear Medicine*, 61(1):144–151, 2020.
- [133] George A Prenosil, Hasan Sari, Markus Fürstner, Ali Afshar-Oromieh, Kuangyu Shi, Axel Rominger, and Michael Hentschel. Performance characteristics of the biograph vision quadra pet/ct system with a long axial field of view using the nema nu 2-2018 standard. *Journal of nuclear medicine*, 63(3):476–484, 2022.
- [134] D Kamińska, Aleksander Gajos, Eryk Czerwiński, Dominika Alfs, Tomasz Bednarski, Piotr Białas, C Curceanu, Kamil Dulski, Bartosz Głowacz, Neha Gupta-Sharma, et al. A feasibility study of ortho-positronium decays measurement with the j-pet scanner based on plastic scintillators. *The European Physical Journal C*, 76:1–14, 2016.
- [135] Pawel Moskal, Daria Kisielewska, Catalina Curceanu, Eryk Czerwiński, Kamil Dulski, Aleksander Gajos, Marek Gorgol, B Hiesmayr, B Jasińska, Krzysztof Kacprzak, et al. Feasibility study of the

- positronium imaging with the j-pet tomograph. *Physics in Medicine & Biology*, 64(5):055017, 2019.
- [136] Hui Tan, Yusen Gu, Haojun Yu, Pengcheng Hu, Yiqiu Zhang, Wujian Mao, and Hongcheng Shi. Total-body pet/ct: current applications and future perspectives. *American Journal of Roentgenology*, 215(2):325–337, 2020.
- [137] Arman Rahmim, Martin A Lodge, Nicolas A Karakatsanis, Vladimir Y Panin, Yun Zhou, Alan McMillan, Steve Cho, Habib Zaidi, Michael E Casey, and Richard L Wahl. Dynamic whole-body pet imaging: principles, potentials and applications. *European journal of nuclear medicine and molecular imaging*, 46:501–518, 2019.
- [138] Szymon Niedzwiecki, Piotr Bialas, Catalina Curceanu, Eryk Czerwinski, Kamil Dulski, Aleksander Gajos, Bartosz Glowacz, M Gorgol, BC Hiesmayr, B Jasinska, et al. J-pet: a new technology for the whole-body pet imaging. *Acta Physica Polonica. B*, 48(1567), 2017.
- [139] Pawel Moskal, Sz Niedzwiecki, Tomasz Bednarski, Eryk Czerwinski, E Kubicz, I Moskal, M Pawlik-Niedzwiecka, NG Sharma, M Silarski, M Zielinski, et al. Test of a single module of the j-pet scanner based on plastic scintillators. *Nuclear Instruments and Methods in Physics Research Section A: Accelerators, Spectrometers, Detectors and Associated Equipment*, 764:317–321, 2014.
- [140] C Grignon, J Barbet, M Bardiès, T Carlier, JF Chatal, O Couturier, Jean-Pierre Cussonneau, A Faivre, L Ferrer, S Girault, et al. Nuclear medical imaging using  $\beta^+$   $\gamma$  coincidences from 44sc radio-nuclide with liquid xenon as detection medium. *Nuclear Instruments and Methods in Physics Research Section A: Accelerators, Spectrometers, Detectors and Associated Equipment*, 571(1-2):142–145, 2007.
- [141] Samuel Duval, Amos Breskin, Herve Carduner, Jean-Pierre Cussonneau, J Lamblin, P Le Ray, E Morteau, T Oger, JS Stutzmann, and D Thers. Mpgds in compton imaging with liquid-xenon. *Journal of Instrumentation*, 4(12):P12008, 2009.
- [142] L Gallego Manzano, JM Abaline, S Acounis, N Beaupère, JL Beney, J Bert, S Bouvier, P Briend, J Butterworth, T Carlier, et al. Xemis2: A liquid xenon detector for small animal medical imaging. *Nuclear Instruments and Methods in Physics Research Section A: Accelerators, Spectrometers, Detectors and Associated Equipment*, 912:329–332, 2018.
- [143] D Giovagnoli, A Bousse, N Beaupere, C Canot, J-P Cussonneau, Sara Diglio, A Iborra Carreres, Julien Masbou, T Merlin, E Morteau, et al. A pseudo-tof image reconstruction approach for three-gamma small animal imaging. *IEEE Transactions on Radiation and Plasma Medical Sciences*, 5(6):826–834, 2020.
- [144] C Lang, D Habs, K Parodi, and PG Thierolf. Submillimeter nuclear medical imaging with reduced dose application in positron emission tomography using  $\beta$   $\gamma$  coincidences. *Preprint Typeset in JINST Style-HYPER VERSION*, 2013.
- [145] Eiji Yoshida, Hideaki Tashima, Kotaro Nagatsu, Atsushi B Tsuji, Kei Kamada, Katia Parodi, and Taiga Yamaya. Whole gamma imaging: a new concept of pet combined with compton imaging. *Physics in Medicine & Biology*, 65(12):125013, 2020.
- [146] Roman Y Shopa and Kamil Dulski. Positronium imaging in J-PET with an iterative activity reconstruction and a multi-stage fitting algorithm. *Bio-Algorithms and Med-Systems*, 19(1):54–63, 2023.
- [147] Roman Y Shopa and Kamil Dulski. Multi-photon time-of-flight mlem application for the positronium imaging in j-pet. *Bio-Algorithms and Med-Systems*, 18(1):135–143, 2022.
- [148] Jinyi Qi and Bangyan Huang. Positronium lifetime image reconstruction for tof pet. *IEEE Transactions on Medical Imaging*, 41(10):2848–2855, 2022.
- [149] Zheyuan Zhu, Chien-Min Kao, and Hsin-Hsiung Huang. A statistical reconstruction algorithm for positronium lifetime imaging using time-of-flight positron emission tomography, 2023.
- [150] Bangyan Huang, Tiantian Li, Gerard Arino-Estrada, Kamil Dulski, Roman Y Shopa, Pawel Moskal, Ewa Stepien, and Jinyi Qi. Split: Statistical positronium lifetime image reconstruction via time-thresholding. *IEEE Transactions on Medical Imaging*, 2024.
- [151] Zhuo Chen, Lingling An, Chien-Min Kao, and Hsin-Hsiung Huang. The properties of the positronium lifetime image reconstruction based on maximum likelihood estimation. *Bio-Algorithms and Med-Systems*, 19(1):1–8, 2023.
- [152] Zhuo Chen, Chien-Min Kao, Hsin-Hsiung Huang, and Lingling An. Enhancing positronium lifetime imaging through two-component reconstruction in time-of-flight positron emission tomography. *arXiv preprint arXiv:2403.14994*, 2024.